

# Facile Estimation of Catalytic Activity and Selectivities in Copolymerization of Propylene Oxide with Carbon Dioxide Mediated by Metal Complexes with Planar Tetradentate Ligand

Takahiro Ohkawara,<sup>†</sup> Kohei Suzuki,<sup>†</sup> Koji Nakano,<sup>‡</sup> Seiji Mori,<sup>\*,§</sup> and Kyoko Nozaki<sup>\*,†</sup>

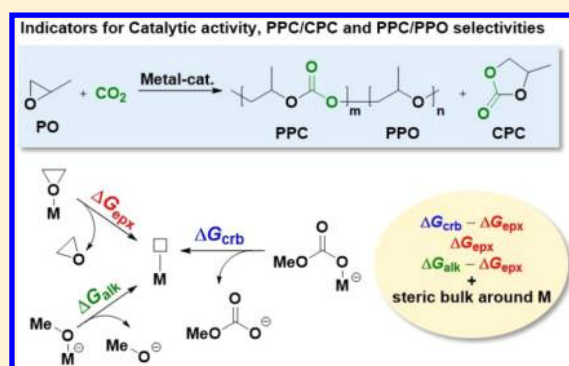
<sup>†</sup>Department of Chemistry and Biotechnology, Graduate School of Engineering, the University of Tokyo 7-3-1 Hongo, Bunkyo-ku, Tokyo 113-8656, Japan

<sup>‡</sup>Department of Organic and Polymer Materials Chemistry, Tokyo University of Agriculture and Technology, 2-24-16 Naka-cho, Koganei, Tokyo 184-8588, Japan

<sup>§</sup>Faculty of Science, Ibaraki University, 2-1-1 Bunkyo, Mito, Ibaraki 310-8512, Japan

## Supporting Information

**ABSTRACT:** Mechanistic studies were conducted to estimate (1) catalytic activity for PPC, (2) PPC/CPC selectivity, and (3) PPC/PPO selectivity for the metal-catalyzed copolymerization of propylene oxide with carbon dioxide [PPC: poly(propylene carbonate); CPC = cyclic propylene carbonate; PPO: poly(propylene oxide)]. Density functional theory (DFT) studies demonstrated that the  $\Delta G_{\text{crb}} - \Delta G_{\text{epx}}$  value should be an effective indicator for the catalytic activities [ $\Delta G_{\text{epx}}$ : dissociation energy of ethylene oxide from the epoxide-coordinating metal complex;  $\Delta G_{\text{crb}}$ : dissociation energy of methyl carbonate from the metal-carbonate complex]. In addition, metal complexes with a subthreshold  $\Delta G_{\text{epx}}$  value were found to show low PPC/CPC selectivity. The PPC/PPO selectivity was related to the  $\Delta G_{\text{alk}} - \Delta G_{\text{epx}}$  value and steric environment around the metal center ( $\Delta G_{\text{alk}}$ : dissociation energy of alkoxide from the metal center). Based on the mechanistic studies, two metal complexes were designed and applied to the copolymerization to support validity of these indicators. The results presented here should be useful for brand-new catalyst candidates since these indicators can be easily calculated by DFT method without computing transition states.



Based on the mechanistic studies, two metal complexes were designed and applied to the copolymerization to support validity of these indicators. The results presented here should be useful for brand-new catalyst candidates since these indicators can be easily calculated by DFT method without computing transition states.

## INTRODUCTION

The epoxide/ $\text{CO}_2$  copolymerization is a promising strategy for  $\text{CO}_2$  utilization, and thus various catalysts have been developed for the copolymerization since the first report by Inoue using heterogeneous zinc catalysts.<sup>1</sup> Among the catalysts so far investigated, recent development of homogeneous metal catalysts is notable as shown in the following examples.<sup>2</sup> Inoue et al. achieved living polymerization using Al-porphyrin complex.<sup>3</sup> Later, since 2000, various new catalyst systems with a well-defined metal complex emerged such as Zn-diiminato<sup>4</sup> and Cr<sup>5</sup> and Co<sup>6</sup>-salen complexes. Thus far, the highest catalytic performance was accomplished by Co-salen complexes; for example, high catalytic activity for poly(propylene carbonate) (PPC) generation and high selectivities for PPC over cyclic carbonate (CPC) and for PPC over poly(propylene oxide) (PPO) were achieved in the propylene oxide (PO)/ $\text{CO}_2$  copolymerization. We have also reported another class of metal catalysts employing trivalent-tetradentate ligands, namely Ti, Ge, and Sn-boxdipy<sup>7</sup> and Fe<sup>8</sup> and Mn<sup>9</sup>-corrole complexes.

Mechanistic studies on the copolymerization were reported for the representative catalysts from both experimental and theoretical viewpoints. Darensbourg and co-workers studied

Cr-salen catalyst system intensively and revealed various properties of the system such as temperature/ $\text{CO}_2$  pressure dependency and the effect of cocatalyst and substituents on the ligand.<sup>5</sup> They also reported mechanistic studies focusing on the decomposition of the product copolymer.<sup>10</sup> Chisholm and co-workers reported a broad range of properties of Al, Cr, and Co-porphyrin and salen catalyst systems. They estimated the order of Lewis acidity of the complexes to be  $\text{Cr(III)} \approx \text{Al(III)} > \text{Co(III)}$  by using electrospray tandem mass spectrometry.<sup>11</sup> They also revealed that the reactivity of (TPP)AlX (TPP = tetraphenylporphyrin and X = Cl, OR, and OCOR) for the PO ring-opening reaction decrease in the order  $\text{Cl} > \text{OR} > \text{O}_2\text{CR}$  in the absence of DMAP (1 equiv) and in the order  $\text{Cl} > \text{OCOR} > \text{OR}$  in the presence of DMAP, respectively.<sup>12</sup> They also found that the rate dependence of the PO ring-opening reaction was first order in [Al]. Elaborate investigation of the catalytic cycle through density functional theory (DFT) studies were also performed for specific catalyst systems based on Zn-

Received: May 17, 2014

Published: July 15, 2014

diiminate,<sup>13</sup> Al and Cr–salen,<sup>14</sup> and dinuclear zinc complexes developed by Williams and co-workers.<sup>15</sup>

As reviewed above, each mechanistic study so far was limited to each family of catalysts, and there has been no report to compare different families of catalysts. In other words, it has not been known why Co–salen catalyst systems show higher performance compared to other systems. This prompted us to develop a common indicator to estimate catalyst performance (catalytic activity, selectivity for PPC/CPC, and selectivity for PPC/PPO). In this work, catalyst systems with M–salen [M = Co (1),<sup>6a,b</sup> Cr (2)<sup>5a,b,d–h</sup>], M–boxdipy<sup>7</sup> [M = Ti (3), Ge (4), Zr (5), Sn (6)], M–corrole [M = Mn (7),<sup>9</sup> Fe (8)<sup>8</sup>], and Al–porphyrin (9)<sup>3</sup> were investigated. All of these complexes possess a planar tetradentate ligand and require cocatalysts such as [PPN]X {[PPN] = bis(triphenylphosphine)iminium} for high catalytic activity (Figure 1). Their catalytic performances

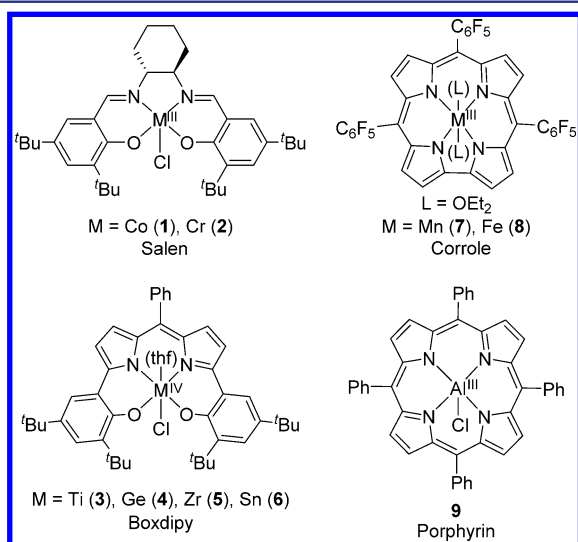


Figure 1. Structures of metal complexes investigated in this work.

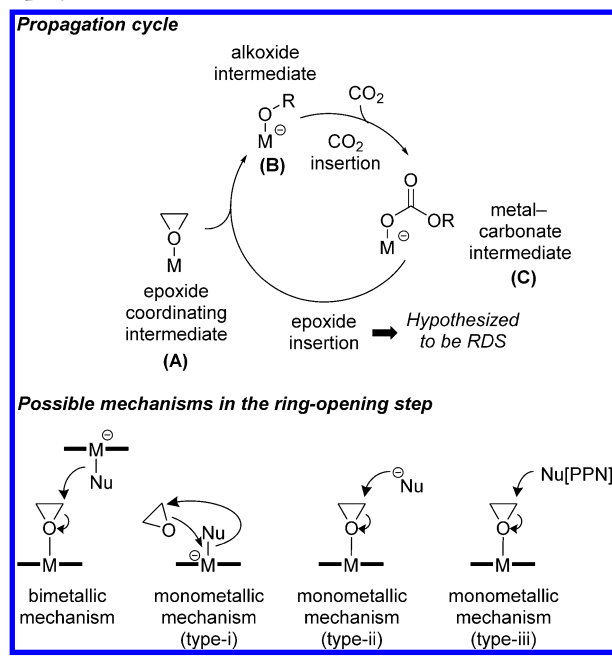
for the PO/CO<sub>2</sub> copolymerization were well-studied. Although there are other highly active catalysts which do not require the cocatalyst or possess different structures, such catalysts are beyond consideration in this work.

## RESULTS AND DISCUSSION

**Indicators for Catalytic Performance.** In this section, we have proposed some indicators to rationalize catalytic activity and selectivities. DFT studies were conducted to estimate Gibbs energies of the key intermediates in the copolymerization. Correlation between the relative Gibbs energy and (1) catalytic activity for PPC generation, (2) PPC/CPC selectivity, and (3) PPC/PPO selectivity were studied. The considerations in this section were applied to the development of new catalysts with higher performance in the following section.

**Activity for PPC Generation.** Chain propagation in the copolymerization consists of two steps. One is the nucleophilic attack of carbonate end on epoxide activated through coordination to the metal center, resulting in a metal–alkoxide intermediate. Another is CO<sub>2</sub> insertion into the metal–alkoxide intermediate to form a metal–carbonate intermediate (Scheme 1). Based on previous reports on several catalyst systems, it should be reasonable to regard the ring-opening of epoxide as a rate-determining step (RDS) in this copolymerization under a wide range of CO<sub>2</sub> pressures.<sup>13,15b,16</sup>

## Scheme 1. Reaction Mechanism of Epoxide/CO<sub>2</sub> Copolymerization



When using metal-complex/[PPN]X catalyst systems, four types of mechanisms may be proposed for the epoxide ring-opening by a nucleophile (Figure 1). The first one is a bimetallic mechanism, where two complexes work cooperatively. Such bimetallic system was proposed for hydrolytic kinetic resolution of epoxides by using a Co–salen complex<sup>17</sup> and for homopolymerization of epoxides catalyzed by a Co–salen complex.<sup>18</sup> The second one is a monometallic mechanism (type i) in which a free epoxide inserts into a metal–nucleophile (Nu) bond, as Darensbourg proposed for the epoxide/CO<sub>2</sub> copolymerization by using Cr–salen/cocatalyst system.<sup>5f</sup> The third and fourth ones (monometallic mechanisms, types ii and iii) are a monometallic mechanism, in which a free nucleophile and [PPN]Nu attacks an epoxide bound to the metal center, respectively. In order to reveal the ring-opening mechanism with metal-complex/[PPN]X catalyst systems, we conducted kinetic studies by using complexes 1, 3, and 4.<sup>19</sup> Reaction orders of 1.57, 1.57, and 1.75 in catalyst concentration were obtained for complexes 1, 3, and 4, respectively, which agree with the result reported in Co–salen/<sup>t</sup>Bu<sub>4</sub>NX catalyst system.<sup>20</sup> This seemed to indicate the complexity of the propagation step, that is, some of four types of mechanism might compete with one another. Nevertheless, in any mechanisms, key species in the epoxide ring-opening step should be the epoxide coordinating intermediate and the nucleophilic carbonate (ROCOO<sup>−</sup>) whether it is free or interacts with the metal center and [PPN] cation.

In order to derive a common indicator for catalytic activities, the dissociation energy of ethylene oxide from the epoxide-coordinating intermediate (A),  $\Delta G_{\text{epx}}$  and the dissociation energy of methyl carbonate from the metal–carbonate intermediate (C),  $\Delta G_{\text{crb}}$ , were computed (Figure 2). The values of  $\Delta G_{\text{epx}}$  and  $\Delta G_{\text{crb}}$  reflect the strength of epoxide–metal and carbonate–metal binding, respectively. These two parameters were compared with the experimental data of the PO/CO<sub>2</sub> copolymerization under the standard reaction conditions (Scheme 2).<sup>21</sup> The theoretical and experimental

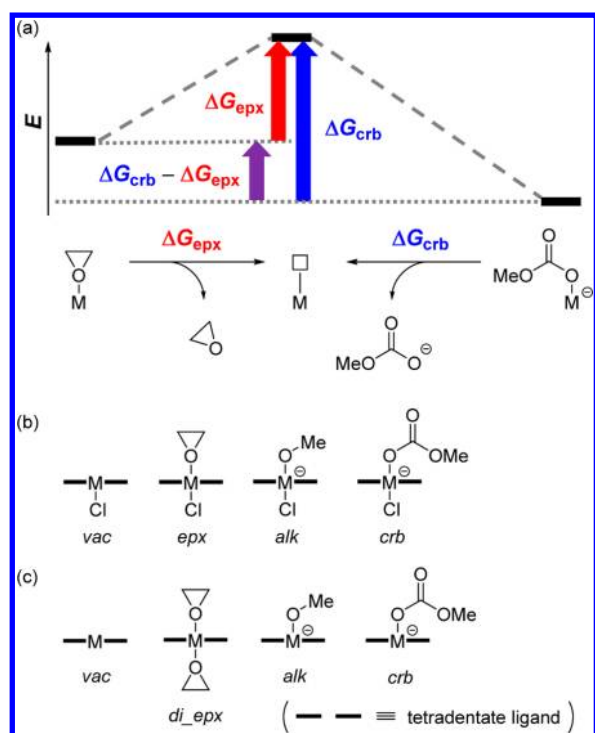
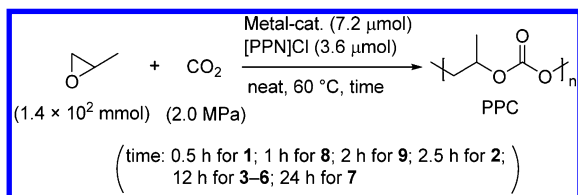


**Figure 2.** (a) Dissociation energies of ethylene oxide ( $\Delta G_{\text{epx}}$ ) and methyl carbonate ( $\Delta G_{\text{crb}}$ ) from metal center, (b) general structures used in calculation for complexes 1–6, 9, and 10, and (c) general structures used in calculation for complexes 7, 8, and 11.

### Scheme 2. Copolymerization of PO with CO<sub>2</sub> by Using Complexes 1–9



results are summarized in Table 1 and Figure 3. Although each parameter  $\Delta G_{\text{epx}}$  or  $\Delta G_{\text{crb}}$  itself did not show any correlation with the catalytic activity [turnover frequency (TOF) for PPC generation], the difference between these two parameters,

**Table 1.** Computed  $\Delta G_{\text{crb}} - \Delta G_{\text{epx}}$  Values and Experimental TOFs for PPC

| complex | $\Delta G_{\text{epx}}$ [kJ/mol] | $\Delta G_{\text{crb}}$ [kJ/mol] | $\Delta G_{\text{crb}} - \Delta G_{\text{epx}}$ [kJ/mol] | TOF for PPC [h <sup>-1</sup> ] |
|---------|----------------------------------|----------------------------------|--|--------------------------------|
| 1       | 11.4                             | 55.5                             | 44.1   | 1144                           |
| 2       | 31.9                             | 87.2                             | 55.3   | 88                             |
| 3       | 22.8                             | 95.9                             | 73.1   | 28                             |
| 4       | 4.8                              | 79.0                             | 74.2   | 14                             |
| 5       | 16.6                             | 106.4                            | 89.8   | 0.7                            |
| 6       | 24.0                             | 93.6                             | 69.6   | 16                             |
| 7       | -2.1                             | 65.3                             | 67.4   | 32                             |
| 8       | 21.1                             | 82.3                             | 61.8   | 230                            |
| 9       | 8.9                              | 70.2                             | 61.3   | 141                            |
| 10      | -4.5                             | 55.4                             | 59.9   | nd <sup>a</sup>                |
| 11      | -10.5                            | 49.5                             | 55.6   | nd <sup>a</sup>                |

<sup>a</sup>nd = not determined because the copolymer was not obtained with complexes 10 and 11.

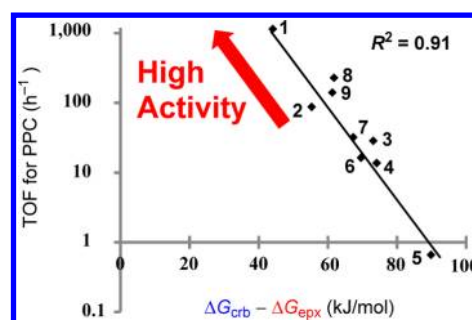


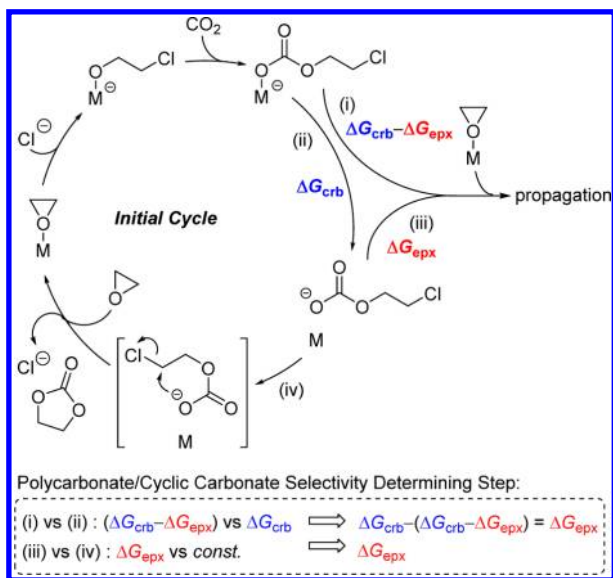
**Figure 3.** Plot of  $\Delta G_{\text{crb}} - \Delta G_{\text{epx}}$  value vs TOF for PPC.

$\Delta G_{\text{crb}} - \Delta G_{\text{epx}}$  and the TOF was found to have a strong negative correlation. Furthermore, the plot of logarithm of TOF vs  $\Delta G_{\text{crb}} - \Delta G_{\text{epx}}$  value showed linear relationship ( $R^2 = 0.91$ ). The parameter  $\Delta G_{\text{crb}} - \Delta G_{\text{epx}}$  corresponds to free energy change in carbonate-epoxide substitution on metal center. Accordingly, it should be regarded as a quantitative indicator for the catalytic activity of the catalyst systems operating in monometallic mechanism. The plot of the data for Fe–corrole catalyst system, which is expected to catalyze the copolymerization via bimetallic mechanism,<sup>22</sup> also follows the linear relationship. Thus, the parameter  $\Delta G_{\text{crb}} - \Delta G_{\text{epx}}$  can be applied to the copolymerization via bimetallic mechanism. In any case, the result described here well matches to our first presumption that the key active species are epoxide-coordinating intermediate (electrophile) and metal–carbonate intermediate (nucleophile).

**PPC/CPC Selectivity.** There should be four species possibly responsible for CPC formation: metal-bound alkoxide, metal-bound carbonate, metal-free alkoxide, and metal-free carbonate. Based on DFT calculations, Rieger and co-workers proposed that the backbiting reaction from a metal-free carbonate end is the main pathway for the CPC formation in the presence of an excess amount of CO<sub>2</sub>.<sup>14</sup> According to our results through in situ IR monitoring, CPC generation mainly occurred at the early stage in the copolymerization (Figure S2). This is probably because the backbiting occurs mainly at the initial step of the copolymerization where the leaving group is Cl<sup>-</sup>; namely, right after nucleophilic attack of the initiator Cl<sup>-</sup> on the first PO and incorporation of the first CO<sub>2</sub>.<sup>10b</sup> This can be rationalized by the fact that chloride is a much better leaving group than alkylcarbonate which is a leaving group in backbiting of elongated polymer chain. Accordingly, the following discussion about the CPC generation is focused on the initial step of the copolymerization, and the mechanism for cyclic carbonate formation is proposed in Scheme 3.

In the proposed mechanism, polycarbonate/cyclic carbonate selectivity should be determined in the two ways. The first one is path (i) vs path (ii), that is, bimolecular nucleophilic attack of metal-bound carbonate end to the activated epoxide vs carbonate dissociation from the metal center. The rate for path (i) depends on the value of  $\Delta G_{\text{crb}} - \Delta G_{\text{epx}}$  (*vide supra*), whereas that for path (ii) can be evaluated by  $\Delta G_{\text{crb}}$  itself. Accordingly, the rate difference between paths (i) and (ii) could be evaluated by  $\Delta G_{\text{epx}}$  [ $\Delta G_{\text{crb}} - (\Delta G_{\text{crb}} - \Delta G_{\text{epx}}) = \Delta G_{\text{epx}}$ ]. The second one is path (iii) vs path (iv), that is, the nucleophilic attack of metal-free carbonate end to the activated epoxide vs the intramolecular backbiting of metal-free carbonate end. The rate for path (iii) could be a function of concentration of epoxide coordinating intermediate, i.e.,  $\Delta G_{\text{epx}}$  whereas the rate of the path (iv) should be less affected by the

Scheme 3. Mechanism for Cyclic Carbonate Formation



catalyst system. Therefore,  $\Delta G_{\text{epx}}$  can be an indicator for the rate difference between paths (iii) and (iv). Accordingly,  $\Delta G_{\text{epx}}$  was regarded as a promising candidate of an indicator for PPC/CPC selectivity.<sup>23</sup>

In contrast to the discussion about catalytic activity for PPC generation, quantitative evaluation of PPC/CPC selectivity seems to be difficult because the CPC generation rate decreases at an early stage in the copolymerization, and thus the PPC/CPC ratio changes continuously over the reaction time (*vide supra*). Therefore, we compared complexes 1–9 with Al (10)<sup>24</sup> and Zn (11)<sup>25</sup> complexes with complete CPC selectivity (Figure 4) to clarify the relationship between the  $\Delta G_{\text{epx}}$  values

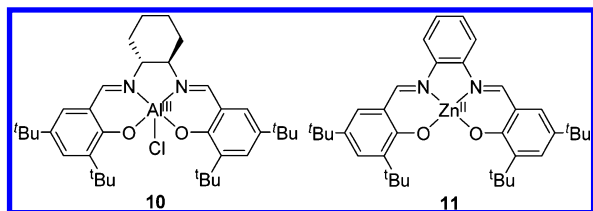
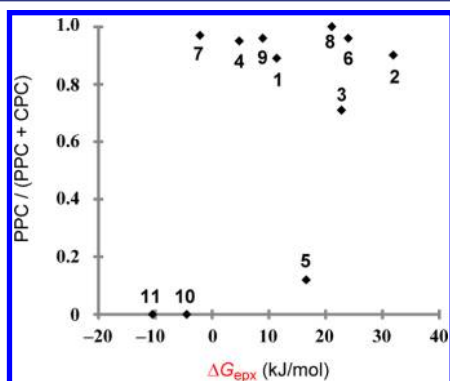


Figure 4. Structures of completely CPC selective catalysts.

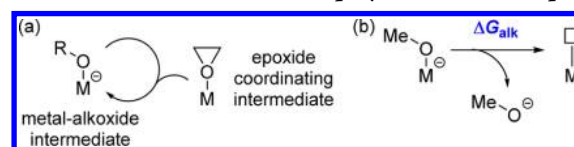
and the PPC/CPC selectivity. As shown in Table 1 and Figure 5, complexes 10 and 11 possess smaller  $\Delta G_{\text{epx}}$  value than

Figure 5. Plot of  $\Delta G_{\text{epx}}$  vs PPC/CPC selectivity.

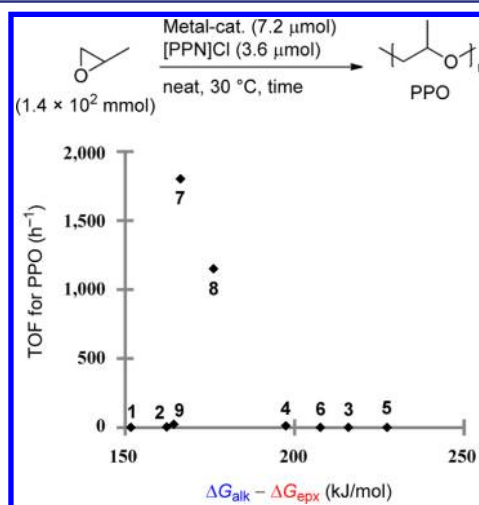
complexes 1–9 and smaller  $\Delta G_{\text{crb}} - \Delta G_{\text{epx}}$  values than complexes 3–9. These results indicate that sufficiently large  $\Delta G_{\text{epx}}$  value is concurrently necessary for PPC generation and high PPC/CPC selectivity even if a complex shows low  $\Delta G_{\text{crb}} - \Delta G_{\text{epx}}$  value.<sup>26</sup>

**PPC/PPO Selectivity.** The PO homopolymerization activity of the complexes was investigated to estimate PPC/PPO selectivity since PPO unit is generated via consecutive insertion of epoxide (Scheme 4a). Catalysts with high PO homopolymer-

Scheme 4. Mechanism for Homopolymerization of Epoxide



ization activity relative to PO/CO<sub>2</sub> copolymerization activity should have low PPC/PPO selectivity. The  $\Delta G_{\text{alk}} - \Delta G_{\text{epx}}$  [ $\Delta G_{\text{alk}}$ : dissociation energy of alkoxide ligand from the metal center (Scheme 4b)] was first investigated as an indicator for PO homopolymerization activity by analogy with the discussion about catalytic activity in the PO/CO<sub>2</sub> copolymerization (*vide supra*). However, no trend was observed in the plot of the  $\Delta G_{\text{alk}} - \Delta G_{\text{epx}}$  value vs the TOF of complexes 1–9 for the PO homopolymerization (Figure 6, Table 2). Complexes 1, 2, and

Figure 6. Plot for  $\Delta G_{\text{alk}} - \Delta G_{\text{epx}}$  vs TOF for PPO.

9 showed low or no activity for the homopolymerization despite the prediction that smaller  $\Delta G_{\text{alk}} - \Delta G_{\text{epx}}$  should provide higher PO homopolymerization activity.

A steric factor was found to correlate with the PPC/PPO selectivity. In contrast that there are several possible mechanisms for polycarbonate formation (Figure 1 and Supporting Information), polyether formation has been mostly proposed to proceed via bimetallic mechanism<sup>27</sup> between epoxide-coordinating species and a nucleophilic metal-alkoxide.<sup>18,28</sup> It should be noted that a bimetallic mechanism in polyether formation requires shorter distance between the two metal centers compared to the polycarbonate formation as illustrated in Figure 7; the metal-bound alkoxide oxygen needs to approach epoxide carbon center in PPO formation, while the carbonate can attack the carbon center through not the metal-bound oxygen but the carbonyl oxygen in PPC formation.

Table 2. Calculated Energies and Experimental PPC/PPO Selectivity<sup>a,b</sup>

| complex | $\Delta G_{\text{alk}}$ [kJ/mol] | $\Delta G_{\text{alk}} - \Delta G_{\text{epx}}$ [kJ/mol] | TOF for PPO [h <sup>-1</sup> ] | $E_{\text{ster}}$ [kJ/mol] | % $V_{\text{Bur}}$ [%] | PPC/PPO |
|---------|----------------------------------|--|--------------------------------|----------------------------|------------------------|---------|
| 1       | 163.1                            | 151.7  | <1                             | 33.2                       | 0.369                  | >99/<1  |
| 2       | 194.2                            | 162.3  | 3.5                            | 31.1                       | 0.367                  | 95/5    |
| 3       | 238.6                            | 215.9  | <1                             | 25.1                       | 0.338                  | 98/2    |
| 4       | 212.4                            | 207.6  | <1                             | 25.9                       | 0.347                  | 89/11   |
| 5       | 243.9                            | 227.3  | <1                             | 18.1                       | 0.377                  | >99/<1  |
| 6       | 221.4                            | 197.4  | 12                             | 15.2                       | 0.314                  | 40/60   |
| 7       | 164.2                            | 166.3  | 1800                           | 9.8                        | 0.263                  | 66/34   |
| 8       | 197.1                            | 176.1  | 1150                           | 12.1                       | 0.273                  | 19/81   |
| 9       | 173.3                            | 164.4  | 24                             | 30.4                       | 0.349                  | 93/7    |

<sup>a</sup>Gibbs energy computed at the B3LYP-D(PCM)/def2-SVP//B3LYP/BI level. <sup>b</sup>Total electronic energy computed at the B3LYP(PCM)/def2-SVP//B3LYP/BI level.

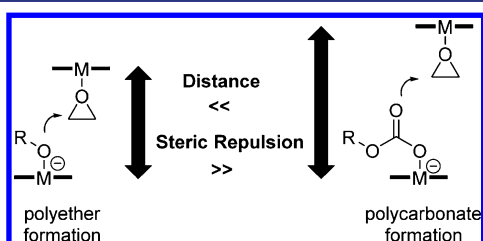


Figure 7. Difference in the distance of two species between polyether formation and polycarbonate formation.

Accordingly, more bulky ligand would make a complex less active for PO homopolymerization and more PPC selective by keeping the two metal centers apart from each other.<sup>29</sup> We hypothesized that bulky environment of complexes 1, 2, and 9 resulted in low PO homopolymerization activity.

In order to evaluate steric environment associated with each ligand, we used two parameters,  $He_8$  steric parameter<sup>30</sup> and percent buried volume.<sup>31</sup> The former parameter was proposed by the Harvey, Orpen, and co-workers to estimate the interaction energy between the phosphorus ligand ( $PA_3$ ) and a planar ring of eight helium atoms which is located 2.28 Å apart from phosphorus atom (Figure 8a). This parameter has

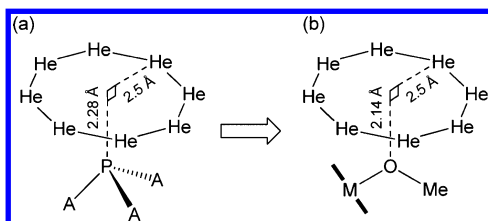


Figure 8. Geometry used for computation of the  $He_8$  steric parameter for (a) phosphorus ligand  $PA_3$  (original one)<sup>30</sup> and (b) metal-alkoxide intermediate (proposed in this work).

the correlation with Tolman cone angle, which is known as a parameter of the steric environment of phosphorus ligands.<sup>32</sup> The latter was proposed by Nolan and co-workers to estimate the steric environment of carbene ligands defined as the percent of the total volume of a sphere occupied by the ligand 2.10 Å apart from the sphere center (Figure 9). These two parameters were employed in our study to evaluate the steric environment of the metal-alkoxide intermediate for complexes 1–9.

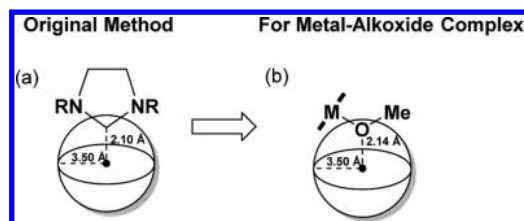


Figure 9. Parameters used for computation of the percent buried volume for (a) NHC ligand (original one)<sup>31</sup> and (b) metal-alkoxide intermediate (proposed in this work).

$He_8$  Steric Parameter. The helium atoms were located in a plane 2.14 Å apart from the alkoxide oxygen. The distance is the average value of the calculated one between alkoxide oxygen and methylene carbon of PO in the transition state of the nucleophilic attack of alkoxide to activated epoxide with bimetallic Co-salen catalyst (Figure 8b).<sup>33</sup> The intermediates were reoptimized in the presence of these He atoms, starting from an optimized conformation of the original complex. The oxygen atom of the alkoxide ligand was constrained to lie exactly 2.14 Å above the ring centroid along the perpendicular to its plane. On the basis of these conditions, interaction energy  $E_{\text{ster}}$  was computed between the intermediate in the ground-state conformation and the ring of eight helium atoms.

Percent Buried Volume. In the same way as for NHC ligands, a sphere with 3.5 Å radius centered at the alkoxide oxygen atom was built to obtain % $V_{\text{Bur}}$  by using free program (see Experimental Section in Supporting Information).

As summarized in Table 2, complexes 1, 2, and 9 showed relatively large value of  $E_{\text{ster}}$  and % $V_{\text{Bur}}$  (Figure S3). This clearly supports our assumption that the sterically hindered environment of these complexes caused low PO homopolymerization activity. In addition, by integrating the discussions above, the combination of (i) small  $\Delta G_{\text{alk}} - \Delta G_{\text{epx}}$  value and (ii) low steric hindrance around the alkoxide oxygen should be necessary for high PO homopolymerization activity. In other words, PPC/PPO selectivity of the complex with these requirements should be lower. This is clearly shown in the plot, where the vertical axis is steric parameter and horizontal axis is the  $\Delta G_{\text{alk}} - \Delta G_{\text{epx}}$  value (Figures 10 and S4). Complexes 6–8 showed lower values for both parameters and actually showed relatively low PPC/PPO selectivity.

The discussion so far clearly showed that the facile estimation for PPC activity, PPC/CPC selectivity, and PPC/

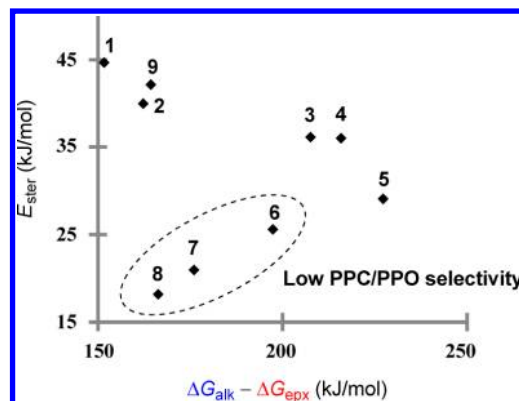
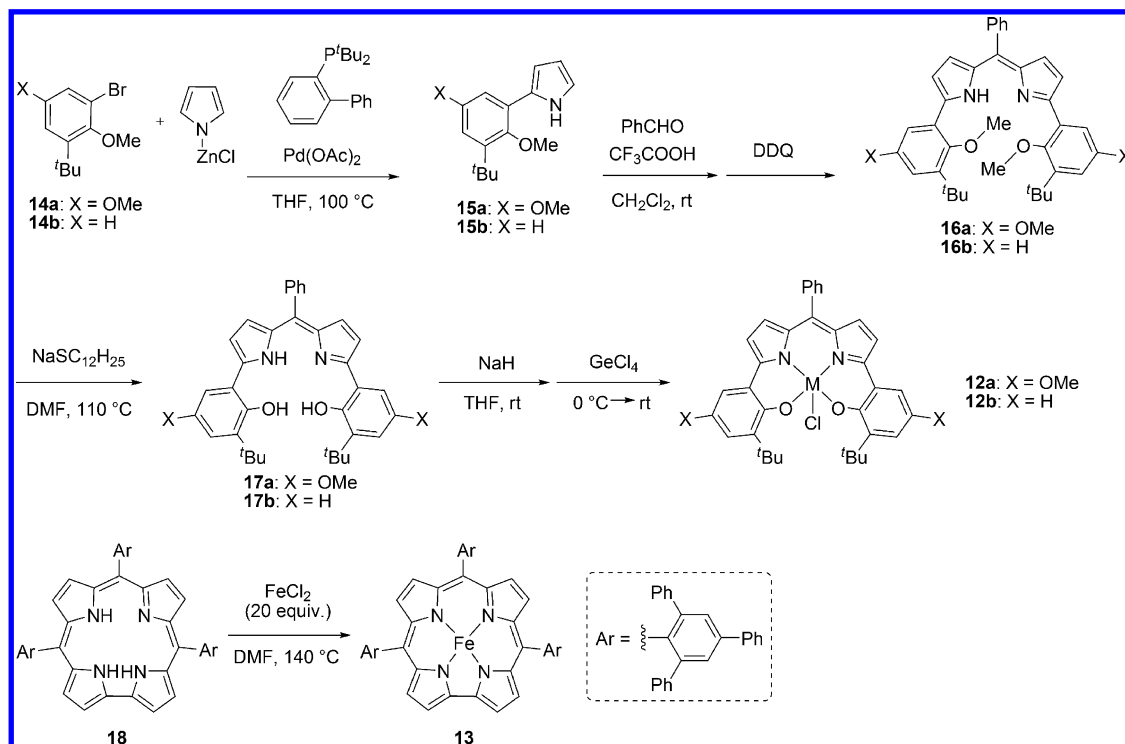


Figure 10. Plot of the  $\Delta G_{\text{alk}} - \Delta G_{\text{epx}}$  value vs  $E_{\text{ster}}$  value.

Scheme 5. Synthesis of Complexes 12 and 13



PPO selectivity was accomplished by simple DFT calculations without transition-state optimizations.

**Development of New Catalysts.** Based on the indicators we proposed above, two types of novel complexes were synthesized (Scheme 5): First one is Ge–boxdipy complexes **12** with substituents X (X = OMe, H) at the *para* position on phenolate moiety, and second one is Fe–corrole complex **13** with bulky substituents. DFT calculations of complexes **12** demonstrated that the  $\Delta G_{\text{crb}} - \Delta G_{\text{epx}}$  values decrease in the order **12b** > **4** > **12a**, and the predicted catalytic activity increases in the order **12b** < **4** < **12a**. This trend can be also interpreted in the way that electron-donating substituents at the *para* position on phenolate moiety improve the catalytic activity. Fe(III)–corrole complex **13** was expected to show improved PPC/PPO selectivity by increasing the steric repulsion, although  $\Delta G_{\text{crb}} - \Delta G_{\text{epx}}$  or  $\Delta G_{\text{alk}} - \Delta G_{\text{epx}}$  could not be computed because of its large number of atoms. Ge–boxdipy complexes were synthesized as shown in Scheme 5. Arylation of pyrrole by 1-bromo-3-*tert*-butyl-2,5-dimethoxybenzene (**14a**)<sup>34</sup> or 1-bromo-3-*tert*-butyl-2-methoxybenzene (**14b**)<sup>35</sup> afforded **15**. Reaction of **15** with benzaldehyde in the presence of catalytic amount of trifluoroacetic acid, and the following oxidation with DDQ gave methyl-protected ligand precursor **16**. Treatment of **16** with an excess amount of sodium thiolate resulted in the selective demethylation of methoxy groups next to *tert*-butyl substituents. The structure of demethylated product **17** was confirmed by X-ray structural analysis (Figure 11). Deprotonation with NaH and subsequent complexation with germanium chloride gave germanium complexes **12**. Fe–corrole complex **13** with bulky substituent was afforded by the reaction of corrole ligand **18**<sup>36</sup> and FeCl<sub>2</sub> in DMF.

The copolymerization of PO with CO<sub>2</sub> was carried out under standard conditions [PO/complex/[PPN]Cl = 2000/1/0.5 ([PPN]Cl = [Ph<sub>3</sub>P=N=PPh<sub>3</sub>]Cl); CO<sub>2</sub> = 2.0 MPa; 60 °C;

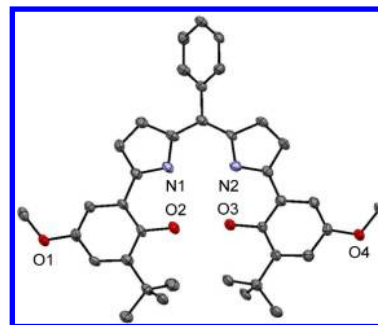
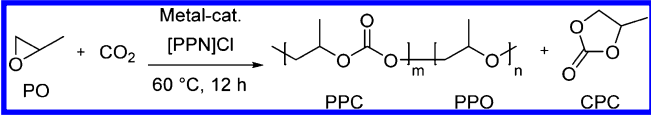


Figure 11. X-ray structure of compound **17a** (hydrogen atoms are omitted for clarity).

12 h]. The results are summarized in Table 3. Ge–boxdipy complex **12a** and **12b** showed higher and lower TOF for PPC generation than complex **4**, respectively (Table 3, entries 1–3). This trend was consistent with the predictions based on the indicator  $\Delta G_{\text{crb}} - \Delta G_{\text{epx}}$ . Accordingly, these results demonstrated that the indicator  $\Delta G_{\text{crb}} - \Delta G_{\text{epx}}$  may be used for prediction of the substituent effect, while the difference is still small. In addition, the order of PPC/PPO selectivity seemed to reflect the steric environment of the complexes. The PPC/PPO selectivity increased in the order **12b** < **12a** < **4** with increase in steric bulkiness at the *para* position on phenolate moiety [H (**12b**) < OMe (**12a**) < *t*Bu (**4**)].

Completely alternating copolymer of PO and CO<sub>2</sub> (Table 3, entry 5) was obtained by using Fe–corrole complex **13** with bulky substituents. The complete PPC/PPO selectivity contrasts with the low PPC/PPO selectivity observed with less bulky complex **8** in our previous study (Table 3, entry 4). This is the first example of completely alternating copolymerization of PO and CO<sub>2</sub> by using iron complexes. Further ligand design for improvement in TOF for PPC and PPC/CPC selectivity is currently in progress.

Table 3. Copolymerization of Propylene Oxide with CO<sub>2</sub> by Using Ge and Fe Complexes<sup>a</sup>


| entry          | complex | yield of copolymer + CPC [%] <sup>b</sup> | copolymer/CPC <sup>b</sup> | TOF for PPC <sup>c</sup> | $\Delta G_{\text{crb}} - \Delta G_{\text{epx}}$ | carbonate linkage [%] <sup>b</sup> | $M_n$ [g·mol <sup>-1</sup> ] <sup>d</sup> | $M_w/M_n$ <sup>d</sup> |
|----------------|---------|---|----------------------------|--------------------------|---|------------------------------------|---|------------------------|
| 1              | 12a     | 12  | 91/9                       | 15                       | 72.7  | 88                                 | 4800                                      | 1.2                    |
| 2              | 4       | 10  | 95/5                       | 14                       | 74.2  | 89                                 | 6000                                      | 1.1                    |
| 3              | 12b     | 7   | 90/10                      | 8                        | 75.6  | 73                                 | 2500                                      | 1.2                    |
| 4 <sup>f</sup> | 8       | 60  | >99/<1                     | 230                      | 61.8  | 19                                 | 39 000                                    | 1.2                    |
| 5              | 13      | 11  | 30/70                      | 5                        | —   | >99                                | 3900                                      | 1.4                    |

<sup>a</sup>PO (1.0 mL, 14.3 mmol), complex 4, 8, 12, or 13 ( $7.0\text{--}7.2 \times 10^{-3}$  mmol), [PPN]Cl ( $3.5\text{--}3.6 \times 10^{-3}$  mmol) in a 50 mL autoclave at 60 °C for 12 h. <sup>b</sup>Determined on the basis of <sup>1</sup>H NMR spectroscopy of the crude product by using phenanthrene as an internal standard. <sup>c</sup>TOF = (mol of carbonate repeating unit)·(mol of complex)<sup>-1</sup>·h<sup>-1</sup>. <sup>d</sup>Determined by size-exclusion chromatography analysis using a polystyrene standard; see ref 7. <sup>f</sup>1 h.

## CONCLUSION

In summary, here we speculated the reaction mechanism of the PPC formation and proposed three indicators for (1) catalytic activity for PPC, (2) PPC/CPC selectivity, and (3) PPC/PPO selectivity. DFT studies afforded an effective indicator,  $\Delta G_{\text{crb}} - \Delta G_{\text{epx}}$ , for the evaluation of the catalytic activities for PPC generation. Furthermore, the  $\Delta G_{\text{epx}}$  itself was found to be an indicator for PPC/CPC selectivity. If  $\Delta G_{\text{epx}}$  is too small, the complex tends to be CPC selective. These indicators can be easily calculated by DFT methods without computing transition states, so that it can be used as a standard when the brand-new catalyst candidates were screened. An indicator,  $\Delta G_{\text{alk}} - \Delta G_{\text{epx}}$  and steric environment around the active center determined the PPC/PPO selectivity. Small  $\Delta G_{\text{alk}} - \Delta G_{\text{epx}}$  and small steric bulk around the metal center facilitate the PPO formation, which resulted in lowering PPC/PPO selectivity.

Two types of metal complexes 12 and 13 were designed based on the parameters above. Copolymerization results with Ge-complexes 12 showed that the proposed indicators can be used to predict the ligand effect. Completely alternating copolymer was given by using Fe-complex 13 owing to its sterically hindered ligand.

Here we presented general explanation for catalytic activity and selectivities common for versatile metal complexes. We believe that this result will give an impact for future catalyst designs.

## ASSOCIATED CONTENT

### Supporting Information

Experimental procedures, consideration on rate-determining step of the copolymerization, real-time IR monitoring, computational methods, crystallographic data, and NMR spectra. This material is available free of charge via the Internet at <http://pubs.acs.org>.

## AUTHOR INFORMATION

### Corresponding Authors

nozaki@chembio.t.u-tokyo.ac.jp  
smori@mx.ibaraki.ac.jp

### Notes

The authors declare no competing financial interest.

## ACKNOWLEDGMENTS

This work was supported by Grant-in-Aid for Scientific Research on Innovative Areas “Molecular Activation Directed

toward Straightforward Synthesis”, No. 23105507 from MEXT to S.M. and K. Nozaki. Partial support to K.Nozaki from Funding Program for Next Generation World-Leading Researchers, Green Innovation and the Global COE Program “Chemistry Innovation through Cooperation of Science and Engineering” from MEXT/JSPS, Japan is also acknowledged. The generous allotment of computation time from the Research Center for Computational Science (RCCS), the National Institutes of Natural Sciences, Japan, is also gratefully acknowledged. We are grateful to Mr. Masahiro Hatazawa, Mr. Ryo Nakano, Dr. Shuhei Kusumoto (U Tokyo) and Mr. Takayoshi Yoshimura (Ibaraki U) for data collections, helpful suggestions, single-crystal X-ray analysis, and DFT setup, respectively.

## REFERENCES

- (1) Inoue, S.; Koinuma, H.; Tsuruta, T. *J. Polym. Sci., Part B: Polym. Lett.* **1969**, *7*, 287–292.
- (2) (a) Darensbourg, D. J. *Chem. Rev.* **2007**, *107*, 2388–2410. (b) Kember, M. R.; Buchard, A.; Williams, C. K. *Chem. Commun.* **2011**, *47*, 141.
- (3) (a) Aida, T.; Inoue, S. *J. Am. Chem. Soc.* **1983**, *105*, 1304–1309. (b) Aida, T.; Inoue, S. *J. Am. Chem. Soc.* **1985**, *107*, 1358–1364. (c) Aida, T.; Sanuki, K.; Inoue, S. *Macromolecules* **1985**, *18*, 1049–1055. (d) Aida, T.; Ishikawa, M.; Inoue, S. *Macromolecules* **1986**, *19*, 8–13. (e) Aida, T.; Inoue, S. *Acc. Chem. Res.* **1996**, *29*, 39–48.
- (4) (a) Cheng, M.; Lobkovsky, E. B.; Coates, G. W. *J. Am. Chem. Soc.* **1998**, *120*, 11018–11019. (b) Cheng, M.; Moore, D. R.; Reczek, J. J.; Chamberlain, B. M.; Lobkovsky, E. B.; Coates, G. W. *J. Am. Chem. Soc.* **2001**, *123*, 8738–8749. (c) Moore, D. R.; Cheng, M.; Lobkovsky, E. B.; Coates, G. W. *Angew. Chem., Int. Ed.* **2002**, *41*, 2599–2602. (d) Allen, S. D.; Moore, D. R.; Lobkovsky, E. B.; Coates, G. W. *J. Am. Chem. Soc.* **2002**, *124*, 14284–14285.
- (5) (a) Darensbourg, D. J.; Yarbrough, J. C. *J. Am. Chem. Soc.* **2002**, *124*, 6335–6342. (b) Darensbourg, D. J.; Yarbrough, J. C.; Ortiz, C.; Fang, C. C. *J. Am. Chem. Soc.* **2003**, *125*, 7586–7591. (c) Darensbourg, D. J.; Rodgers, J. L.; Fang, C. C. *Inorg. Chem.* **2003**, *42*, 4498–4500. (d) Darensbourg, D. J.; Mackiewicz, R. M.; Rodgers, J. L.; Fang, C. C.; Billodeaux, D. R.; Reibenspies, J. H. *Inorg. Chem.* **2004**, *43*, 6024–6034. (e) Darensbourg, D. J.; Mackiewicz, R. M.; Rodgers, J. L.; Phelps, A. L. *Inorg. Chem.* **2004**, *43*, 1831–1833. (f) Darensbourg, D. J.; Mackiewicz, R. M. *J. Am. Chem. Soc.* **2005**, *127*, 14026–14038. (g) Darensbourg, D. J.; Phelps, A. L. *Inorg. Chem.* **2005**, *44*, 4622–4629. (h) Darensbourg, D. J.; Mackiewicz, R. M.; Billodeaux, D. R. *Organometallics* **2005**, *24*, 144–148.
- (6) (a) Qin, Z.; Thomas, C. M.; Lee, S.; Coates, G. W. *Angew. Chem., Int. Ed.* **2003**, *42*, 5484–5487. (b) Cohen, C. T.; Chu, T.; Coates, G. W. *J. Am. Chem. Soc.* **2005**, *127*, 10869–10878. (c) Cohen, C. T.; Thomas, C. M.; Peretti, K. L.; Lobkovsky, E. B.; Coates, G. W. *Dalton*

*Trans.* **2006**, 237–249. (d) Cohen, C. T.; Coates, G. W. *J. Polym. Sci., Part A: Polym. Chem.* **2006**, 44, 5182–5191. (e) Lu, X. B.; Wang, Y. *Angew. Chem., Int. Ed.* **2004**, 43, 3574–3577. (f) Noh, E. K.; Na, S. J.; Sujith, S.; Kim, S. W.; Lee, B. Y. *J. Am. Chem. Soc.* **2007**, 129, 8082–8083. (g) Sujith, S.; Min, K. K.; Seong, J. E.; Na, S. J.; Lee, B. Y. *Angew. Chem., Int. Ed.* **2008**, 47, 7306–7309. (h) Ren, W.-M.; Liu, Z.-W.; Wen, Y.-Q.; Zhang, R.; Lu, X.-B. *J. Am. Chem. Soc.* **2009**, 131, 11509–11518.

(7) Nakano, K.; Kobayashi, K.; Nozaki, K. *J. Am. Chem. Soc.* **2011**, 133, 10720–10723.

(8) Nakano, K.; Kobayashi, K.; Ohkawara, T.; Imoto, H.; Nozaki, K. *J. Am. Chem. Soc.* **2013**, 135, 8456–8459.

(9) Robert, C.; Ohkawara, T.; Nozaki, K. *Chem.—Eur. J.* **2014**, 20, 4789–4795.

(10) (a) Darensbourg, D. J.; Wei, S.-H. *Macromolecules* **2012**, 45, 5916–5922. (b) Darensbourg, D. J.; Yeung, A. D. *Macromolecules* **2013**, 46, 83–95. (c) Darensbourg, D. J.; Yeung, A. D.; Wei, S.-H. *Green Chem.* **2013**, 15, 1578–1583.

(11) Chen, P.; Chisholm, M. H.; Gallucci, J. C.; Zhang, X.; Zhou, Z. *Inorg. Chem.* **2005**, 44, 2588–2595.

(12) Chisholm, M. H.; Zhou, Z. *J. Am. Chem. Soc.* **2004**, 126, 11030–11039.

(13) Liu, Z.; Torrent, M.; Morokuma, K. *Organometallics* **2002**, 21, 1056–1071.

(14) Luinstra, G. A.; Haas, G. R.; Molnar, F.; Bernhart, V.; Eberhardt, R.; Rieger, B. *Chem.—Eur. J.* **2005**, 11, 6298–6314.

(15) (a) Lehenmeier, M. W.; Bruckmeier, C.; Klaus, S.; Dengler, J. E.; Deglmann, P.; Ott, A.-K.; Rieger, B. *Chem.—Eur. J.* **2011**, 17, 8858–8869. (b) Buchard, A.; Jutz, F.; Kember, M. R.; White, A. J. P.; Rzepa, H. S.; Williams, C. K. *Macromolecules* **2012**, 45, 6781–6795.

(16) (a) Moore, D. R.; Cheng, M.; Lobkovsky, E. B.; Coates, G. W. *J. Am. Chem. Soc.* **2003**, 125, 11911–11924. (b) Kember, M. R.; White, A. J. P.; Williams, C. K. *Macromolecules* **2010**, 43, 2291–2298.

(17) Tokunaga, M.; Larrow, J. F.; Kakiuchi, F.; Jacobsen, E. N. *Science* **1997**, 277, 936–938.

(18) Hirahata, W.; Thomas, R. M.; Lobkovsky, E. B.; Coates, G. W. *J. Am. Chem. Soc.* **2008**, 130, 17658–17659.

(19) See the Supporting Information for the detail of kinetic study.

(20) Liu, J.; Ren, W.-M.; Liu, Y.; Lu, X.-B. *Macromolecules* **2013**, 46, 1343–1349.

(21) The TOF represents a composite of the rate of initiation and propagation. Our *in situ* IR monitoring of the PO/CO<sub>2</sub> copolymerization with complexes **1**, **3**, **4**, and **8** revealed that the initiation periods were negligibly short compared with the total copolymerization periods and that the propagation proceeded at the same rate from very early period during the copolymerization. Accordingly, the TOF are used as the propagation rate in this work.

(22) The Fe–corrole catalyst system demonstrated the highest activity by the addition of 0.50 equiv of [PPN]Cl to Fe, while the addition of 1.0 equiv of [PPN]Cl diminished the catalytic activity significantly. This result indicates the copolymerization proceeded via bimetallic mechanism, see ref 8.

(23) Bifunctional Co–salen catalyst systems with intramolecular ammonium moieties demonstrated high PPC/CPC selectivity.<sup>6f–h</sup> The high selectivity should be attributed to the capture of metal-free carbonate end with the ammonium moieties, which affect the rate of the path (iv). Accordingly, bifunctional systems were not studied in this work.

(24) (a) Tian, D.; Liu, B.; Gan, Q.; Li, H.; Darensbourg, D. J. *ACS Catal.* **2012**, 2, 2029–2035. (b) Darensbourg, D. J.; Billodeaux, D. R. *Inorg. Chem.* **2005**, 44, 1433–1442.

(25) (a) Decortes, A.; Martínez Belmonte, M.; Benet-Buchholz, J.; Kleij, A. W. *Chem. Commun.* **2010**, 46, 4580. (b) Taherimehr, M.; Decortes, A.; Al-Amsyar, S. M.; Lueangchaichaweng, W.; Whiteoak, C. J.; Escudero-Adan, E. C.; Kleij, A. W.; Pescarmona, P. P. *Catal. Sci. Technol.* **2012**, 2, 2231–2237. (c) Castro-Gómez, F.; Salassa, G.; Kleij, A. W.; Bo, C. *Chem.—Eur. J.* **2013**, 19, 6289–6298.

(26) The low selectivity of complex **5** in spite of its relatively large  $\Delta G_{\text{epx}}$  value may be attributed to its low catalytic activity. That is, the

contribution of other pathways for CPC generation becomes larger which does not show large effect for other catalysts, such as a backbiting of metal-coordinating carbonate.

(27) For Al–porphyrin complex, monometallic mechanism was proposed; see ref 12.

(28) Braune, W.; Okuda, J. *Angew. Chem., Int. Ed.* **2003**, 42, 64–68.

(29) The size of the substituent on ligand was found to affect the ring-opening transition state in (salen)Co-catalyzed epoxide hydrolysis via bimetallic mechanism; see: Ford, D. D.; Nielsen, L. P. C.; Zuend, S. J.; Musgrave, C. B.; Jacobsen, E. N. *J. Am. Chem. Soc.* **2013**, 135, 15595–15608.

(30) Fey, N.; Tsipis, A. C.; Harris, S. E.; Harvey, J. N.; Orpen, A. G.; Mansson, R. A. *Chem.—Eur. J.* **2006**, 12, 291–302.

(31) Hillier, A. C.; Sommer, W. J.; Yong, B. S.; Petersen, J. L.; Cavallo, L.; Nolan, S. P. *Organometallics* **2003**, 22, 4322–4326.

(32) Tolman, C. A. *Chem. Rev.* **1977**, 77, 313–348.

(33) Ahmed, S. M.; Poater, A.; Childers, M. L.; Widger, P. C. B.; LaPointe, A. M.; Lobkovsky, E. B.; Coates, G. W.; Cavallo, L. *J. Am. Chem. Soc.* **2013**, 117, 18901–18911.

(34) Johansson, H.; Shanks, D.; Engman, L.; Amorati, R.; Pedulli, G. F.; Valgimigli, L. *J. Org. Chem.* **2010**, 75, 7535–7541.

(35) Gruza, M. M.; Chambron, J.-C.; Espinosa, E.; Aubert, E. *Eur. J. Org. Chem.* **2009**, 2009, 6318–6327.

(36) Liu, H.-Y.; Yam, F.; Xie, Y.-T.; Li, X.-Y.; Chang, C. K. *J. Am. Chem. Soc.* **2009**, 131, 12890–12891.